

# Distinguishing $Z'$ signatures and the Littlest Higgs model in $e^+e^-$ Colliders at $\sqrt{s} \neq M_{Z'}$

F. M. L. de Almeida Jr., Y. A. Coutinho,  
J. A. Martins Simões, A. J. Ramalho, S. Wulck  
*Instituto de Física,  
Universidade Federal do Rio de Janeiro,  
Rio de Janeiro, RJ, Brazil\**

M. A. B. do Vale  
*Departamento de Ciências Naturais,  
Universidade Federal de São João del Rei,  
São João del Rei, MG, Brazil †*

(Dated: April 16, 2018)

There is a recent proposal identifying the Higgs particle of the Standard Model as a pseudo Nambu-Goldstone boson. This new broken symmetry introduces new particles and new interactions. Among these new interactions a central role to get a new physics is played by two new heavy neutral gauge bosons. We have studied the two new neutral currents in the Littlest Higgs model and compared with other extended models. For high energy  $e^+e^-$  colliders we present a clear signature for these two new neutral gauge bosons that can indicate the theoretical origin of these particles. Previous analysis by other authors were done at collider energies equal to the new gauge boson mass  $M_{A_H}$ . In this paper we show that asymmetries in fermion antifermion production can display model differences in the case  $M_{A_H} > \sqrt{s}$ . For  $M_{A_H} < \sqrt{s}$  we show that the hard photon energy distribution in  $e^+ + e^- \rightarrow \gamma + f + \bar{f}$  can present a model dependence. For higher energies, the hard photon energy distribution can be a clear signature for both new neutral gauge bosons. New bounds for the new neutral gauge boson masses are also presented.

PACS numbers: 12.60.Nz,14.80.Mz,13.66.Hk

## I. INTRODUCTION

The Higgs divergent radiative corrections indicate that the Standard Model (SM) is an effective field theory, valid up to a scale  $\Lambda$ . The excellent agreement between the theory and experiment fixes this scale on a few TeV. Above this scale a new theory must solve the hierarchy problem. One possible solution to this problem was recently given by the called Little Higgs models [1]. In these models, the Standard Model Higgs particle is viewed as a pseudo-Goldstone boson of a new global symmetry group. In a first stage, this symmetry is spontaneously broken and the Higgs is a massless particle. A new "collective" symmetry breaking gives a mass to the Higgs boson. The net result is that the new particles and couplings cancel exactly the awful behavior of the Standard Model divergent diagrams giving a light mass to the Higgs fields. Recently, several proposals for "Little Higgs" models have been made. Their main difference are the choice of the new global symmetry. One explicit model [2], with fewer number of new parameters as possible, was named as the "Littlest Higgs model" (here after LHM). It is constructed using an  $SU(5)/S0(5)$  coset: a gauged  $(SU(2) \otimes U(1))^2$  is broken to its subgroup  $SU(2)_L \otimes U(1)_Y$ . A detailed study of this model was done in reference [3] and some more general reviews are given in [4, 5]. The earlier versions of the LHM presented some difficulties. From the analysis of the electroweak precision constraints it was shown [6] that a fine tuning was necessary

---

\*Electronic address: marroqui@if.ufrj.br, yara@if.ufrj.br, simoes@if.ufrj.br, ramalho@if.ufrj.br, steniow@if.ufrj.br

†Electronic address: aline@ufsj.edu.br

in order to get a Higgs mass of 200 GeV. The main problem could be related to the large top Yukawa coupling that generates instabilities in the Higgs potential. Some modifications were introduced such as a new single U(1) [7] and T-parity [8, 9, 10]. The important point in these extensions is that the scale parameter that fixes the LHM could be as low as  $f > 450$  GeV instead of  $f \simeq 10$  TeV. This point re-opened the possibility of testing the LHM at the LHC energies. Many proposed models predict the existence of an extra heavy neutral gauge boson,  $Z'$ . These include: 3-3-1 models [11, 12], little Higgs model [13], left-right symmetric models [14], supersymmetric breaking with an extra non-anomalous U(1) [15], superstring inspired E6 model [16] and models with extra dimensions as Kaluza-Klein excitations of neutral gauge bosons [17].

The experimental verification of these models, and alternatives like supersymmetric models, could be done by the small quantum corrections to the SM predictions and/or by the discovery of new particles. This will be the main task of the high energy and luminosity accelerators LHC and ILC. Since there are many models with new interactions and particles, it will be necessary to have very clear signatures to distinguish the available models. From the experimental point of view a fundamental question is the nature and properties of the lightest particle in extended models. In the LHM this particle is a new neutral gauge boson, named  $A_H$ . A simple and unique property of this model is the presence of a second, heavier, new neutral gauge boson, named  $Z_H$  with correlated masses. These new neutral heavy gauge bosons ( named in general here as  $Z'$  ) could be found in the next generation of high energy colliders: hadron + hadron  $\rightarrow Z' \rightarrow \ell^+ + \ell^-$  and  $e^+ + e^- \rightarrow Z' \rightarrow \ell^+ + \ell^-$  ( with  $\ell = e, \mu, \tau$  ). These topics have been studied by many authors during the last years [18, 19]. It is expected that at the LHC energies the new neutral gauge bosons will give detectable signals or new mass limits for the  $Z'$  and that at future high energy electron-positron colliders it will be possible to study its properties, in details.

The center-of-mass energy of the future colliders will be set to the highest possible values, consistent with technical feasibility and cost limits. However it is also possible that the masses of the new particles will be below the initially designed collider energy. Another fundamental point is that the little Higgs models, as well as practically all other extended model with a new neutral gauge boson, have at least two unknown parameters: the new mass value and some mixing parameter(s) in the coupling with standard matter. The optimistic view that a new neutral current experimental signal will be seen at the LHC and more precisely studied at a new lepton collider will probably show that many extended model could account for this signal. But the LHM has another fundamental feature: a second, heavier, new neutral gauge boson. As cross sections at the resonant energies have the highest possible values it will be necessary to recalibrate the whole collider in order to fix its CM energy at the new resonant mass. Although physically well motivated, this procedure could be time-consuming and costly. It is important to have simple alternative signatures in order to show model differences already in the initial collider working period. Earlier works on the LHM have started from the possibility of a first experimental signature for new gauge interactions at the LHC and then the leptonic colliders were considered at a fixed center of mass energy equal to the new boson mass values [20].

The main point proposed in this paper is that it is not necessary to wait until the lepton collider energy could be fixed at the mass of the new neutral gauge boson in order to get its properties and exclude some models. We will consider new bounds and model differences of new neutral gauge bosons for different  $\sqrt{s}$  values, taking  $\sqrt{s} \neq M_{Z'}$ , both for polarized and unpolarized beams. The other difference with previous works [21, 22] is that we will consider as a signature for new neutral gauge bosons the process  $e^+ + e^- \rightarrow \mu^+ + \mu^- + \gamma$ , where the final state photon is a hard photon with  $E_\gamma > 50$  GeV [23].

In this paper we will discuss these two main signatures for electron-positron colliders that can point to model differences: asymmetries in the production of fermion pairs and the production of a single hard photon associated with new heavy neutral gauge bosons. Total cross sections will be shown to present detectable effects. The fermion pair production allows one to find new limits that can be model dependent for  $M_{Z'} > \sqrt{s}$  and the hard photon production allows one to study the region for  $M_{Z'} < \sqrt{s}$ .

We concentrate our attention first on the lightest neutral gauge boson of the LHM -  $A_H$ . The present experimental limit is  $M_{A_H} > 600$  GeV obtained by [24] and is somewhat model dependent. The other neutral gauge boson  $Z_H$  is heavier, with a mass of the order  $M_{Z_H} \simeq 4M_{A_H}$ . In Section 2 we briefly review the models considered in this paper.

	$g_V$	$g_A$
$A_H \bar{e}e$	$\bar{g}(2y_e - \frac{9}{5} + \frac{3 \cos^2 \theta'}{2})$	$\bar{g}(-\frac{1}{5} + \frac{\cos^2 \theta'}{2})$
$A_H \bar{\nu}_e \nu_e$	$\bar{g}(y_e - \frac{4}{5} + \frac{\cos^2 \theta'}{2})$	$\bar{g}(-y_e + \frac{4}{5} - \frac{\cos^2 \theta'}{2})$
$A_H \bar{u}u$	$\bar{g}(2y_u + \frac{17}{15} - \frac{5 \cos^2 \theta'}{6})$	$\bar{g}(\frac{1}{5} - \frac{\cos^2 \theta'}{2})$
$A_H \bar{d}d$	$\bar{g}(2y_u + \frac{11}{15} + \frac{\cos^2 \theta'}{6})$	$\bar{g}(-\frac{1}{5} + \frac{\cos^2 \theta'}{2})$
$A_H \bar{t}t$	$\bar{g}(2y_u + \frac{17}{15} - \frac{5 \cos^2 \theta'}{6} - \frac{x_L}{5})$	$\bar{g}(\frac{1}{5} - \frac{\cos^2 \theta'}{2} - \frac{x_L}{5})$

TABLE I: Couplings between  $A_H$  and fermions in LHM, with  $\bar{g} = \frac{g'}{2 \sin \theta' \cos \theta'}$  where  $\theta'$  is the mixing angle.

In Section 3 we present our results on the asymmetries. The new bounds on the LHM parameters are displayed in Section 4, and a new signature for the  $A_H$  and  $Z_H$  bosons in Section 5. Finally, in Section 6, we give our final conclusions.

## II. THE MODELS

In order to compare the LHM predictions with other models we will employ the canonical  $\eta, \chi, \psi$  superstring inspired  $E_6$  models [24], Symmetric Left-Right model (SLRM) and Mirror Left-Right Model (MLRM) [23]. As our main interest is the detection of new gauge bosons, we will consider only their coupling to ordinary matter. New particle states must also be coupled to new gauge bosons but this will introduce new parameters and will make the estimates more model dependent in the order hand this will demand also a more sophisticated experimental analysis.

The general form of the interaction Lagrangian involving only ordinary fermions and extra neutral gauge bosons is given by

$$\mathcal{L} = \bar{\Psi} \gamma_\mu (g_V - g_A \gamma_5) \Psi Z'^\mu. \quad (1)$$

where  $g_V$  and  $g_A$  are respectively the vector and vector-axial couplings. The  $\gamma$  and  $Z$  couplings to the ordinary matter are the same as the SM ones.

For the LHM, according to reference [3], the new neutral gauge bosons  $A_H$  and  $Z_H$  couple with ordinary matter with mixing angles  $\theta'$  and  $\theta$  respectively. The couplings are shown in Tables I and II, where  $g$  and  $g'$  are the constant couplings group,  $y_u = -2/5$  and  $y_e = 3/5$  are hypercharges and  $x_L = \lambda_1^2 / (\lambda_1^2 + \lambda_2^2)$ , are combinations of the coupling parameters  $\lambda_1 = 1$  and  $\lambda_2 = 2$ .

The superstring inspired  $E_6$  models [24]  $\eta, \chi, \psi$  have only a new neutral gauge boson  $Z'$  coupled to fermions, as shown in Table III.

	$g_V$	$g_A$
$Z_H \bar{e}e$	$-\frac{g \cos \theta}{4 \sin \theta}$	$-\frac{g \cos \theta}{4 \sin \theta}$
$Z_H \bar{\nu}_e \nu_e$	$\frac{g \cos \theta}{4 \sin \theta}$	$\frac{g \cos \theta}{4 \sin \theta}$
$Z_H \bar{u}u$	$\frac{g \cos \theta}{4 \sin \theta}$	$\frac{g \cos \theta}{4 \sin \theta}$
$Z_H \bar{d}d$	$-\frac{g \cos \theta}{4 \sin \theta}$	$-\frac{g \cos \theta}{4 \sin \theta}$

TABLE II: Couplings between  $Z_H$  and fermions in Little Higgs model where  $\theta$  is the mixing angle.

	$\chi$ -Model		$\eta$ -Model		$\psi$ -Model	
	$g_V$	$g_A$	$g_V$	$g_A$	$g_V$	$g_A$
$Z' \bar{e}e$	$-\frac{g \tan \theta_W}{\sqrt{6}}$	$-\frac{g \tan \theta_W}{2\sqrt{6}}$	$-\frac{g \tan \theta_W}{4}$	$-\frac{g \tan \theta_W}{12}$	0	$\frac{-g \tan \theta_W \sqrt{10}}{12}$
$Z' \bar{\nu}_e \nu_e$	$-\frac{3g \tan \theta_W}{4\sqrt{6}}$	$-\frac{3g \tan \theta_W}{4\sqrt{6}}$	$-\frac{g \tan \theta_W}{12}$	$-\frac{g \tan \theta_W}{12}$	$-\frac{g \tan \theta_W \sqrt{10}}{24}$	$-\frac{g \tan \theta_W \sqrt{10}}{24}$
$Z' \bar{u}u$	0	$\frac{g \tan \theta_W}{2\sqrt{6}}$	0	$\frac{g \tan \theta_W}{3}$	0	$\frac{-g \tan \theta_W \sqrt{10}}{12}$
$Z' \bar{d}d$	$\frac{g \tan \theta_W}{\sqrt{6}}$	$-\frac{g \tan \theta_W}{2\sqrt{6}}$	$\frac{g \tan \theta_W}{4}$	$\frac{g \tan \theta_W}{12}$	0	$\frac{-g \tan \theta_W \sqrt{10}}{12}$

TABLE III: Couplings between  $Z'$  and fermions in  $\psi$ ,  $\eta$  and  $\chi$  models where  $\theta_W$  is the Weinberg angle.

For the Symmetrical and Mirror left-right models, the couplings between fermions and the only extra neutral gauge boson  $Z'$  are presented in Table IV.

Fermion Mirror Fermion Model			Symmetric Model	
	$g_V$	$g_A$	$g_V$	$g_A$
$Z'\bar{e}e$	$\frac{3g \tan \theta_W \tan \beta}{4}$	$-\frac{g \tan \theta_W \tan \beta}{4}$	$\frac{g(-1 + 4 \sin^2 \theta_W)}{4 \cos \theta_W \sqrt{\cos 2\theta_W}}$	$\frac{g \cos 2\theta_W}{4 \cos \theta_W \sqrt{\cos 2\theta_W}}$
$Z'\bar{\nu}_e \nu_e$	$\frac{g \tan \theta_W \tan \beta}{4}$	$\frac{g \tan \theta_W \tan \beta}{4}$	$\frac{g}{4 \cos \theta_W \sqrt{\cos 2\theta_W}}$	$-\frac{g \cos 2\theta_W}{4 \cos \theta_W \sqrt{\cos 2\theta_W}}$
$Z'\bar{u}u$	$-\frac{5g \tan \theta_W \tan \beta}{12}$	$\frac{3g \tan \theta_W \tan \beta}{12}$	$\frac{g(3 - 8 \sin^2 \theta_W)}{12 \cos \theta_W \sqrt{\cos 2\theta_W}}$	$\frac{-3g \cos 2\theta_W}{12 \cos \theta_W \sqrt{\cos 2\theta_W}}$
$Z'\bar{d}d$	$\frac{g \tan \theta_W \tan \beta}{12}$	$-\frac{3g \tan \theta_W \tan \beta}{12}$	$\frac{g(-3 + 4 \sin^2 \theta_W)}{12 \cos \theta_W \sqrt{\cos 2\theta_W}}$	$\frac{3g \cos 2\theta_W}{12 \cos \theta_W \sqrt{\cos 2\theta_W}}$

TABLE IV: Couplings between  $Z'$  and fermions in Symmetric and Mirror left-right models.  $\theta_W$  is the Weinberg angle and  $\sin^2 \beta = \frac{g^2}{g_R^2 + g^2}$  where  $g$  and  $g_R$  are the gauge constant couplings.

### III. ASYMMETRIES

The angular asymmetry is an interesting variable because it is strongly dependent on the couplings  $g_V$  and  $g_A$ . The leptonic asymmetries for the process  $e^+ + e^- \rightarrow \mu^+ + \mu^-$  presented in [25, 26] were calculated for  $\sqrt{s} \simeq M_{A_H}$  where  $M_{A_H}$  is the lightest new neutral boson mass. In this paper, we consider the same channel but for new gauge boson mass regions below and above the collider energy. In all calculations, each final lepton was required to be detected within the azimuthal angle range  $|\cos \phi| < 0.995$ , where  $\phi$  is the angle of either of the final fermions with respect to the direction of the electron beam. This cut corresponds roughly to the detector limitations. For the LHM, the total width  $\Gamma_{A_H}$  was calculated considering the main contributions from pairs of ordinary charged and neutral fermions and  $A_H$ - $Z$ - $H$  couplings. For the  $\Gamma_{Z_H}$  width we have included these channels and the relevant contribution from  $W^+W^-$  channel, which is negligible for  $A_H$ . The mass relation between  $A_H$  and  $Z_H$  is approximately given by the relation  $M_{Z_H} \simeq \sqrt{5}M_{A_H}/\tan \theta_W$ . As a consequence, in the energy region from 500 GeV to 1 TeV the processes will be dominated by  $Z$  and  $A_H$  exchange, if we assume  $M_{A_H} > 500$  GeV. Typical values for the widths, for a choice  $c \equiv \cos \theta = 0.3$ ,  $c' \equiv \cos \theta' = 0.62$ , give us  $\Gamma_{Z_H} = 11$  GeV for  $M_{Z_H} = 2.4$  TeV and  $\Gamma_{A_H} = 0.07$  GeV for  $M_{A_H} = 500$  GeV, in accordance with the results in reference [3].

A first result involving LHM parameters is the total cross section for  $e^+ + e^- \rightarrow \mu^+ + \mu^-$  as a function of the  $\sqrt{s}$ , for  $M_{A_H} = 500$  GeV and  $M_{A_H} = 800$  GeV. The curves are shown in Figure 1. As expected, near the resonant region there is a peak related to the extra gauge boson exchange. We have considered the mixing angles  $\theta$  and  $\theta'$  in the ranges of 0 - 0.5 and 0.62 - 0.73, respectively, as allowed by the precision electroweak constrains on the parameter space of the LHM [6].

A first difference between the theoretical models can be found in the forward-backward asymmetries ( $A_{FB}$ ) in  $e^+ + e^- \rightarrow f + \bar{f}$ , with  $f = \mu^-, c$  and  $b$ . These fermion couplings to  $A_H$  allow a clear model separation from other extended models. We have performed the calculation with the CompHep package [27], in which the previously mentioned models were implemented. The curves for  $A_{FB}$  are displayed in Figures 2,3 and 4 for the models cited above: LHM with a choice of the mixing parameters  $c, c'$ ; superstring inspired models  $\eta, \chi, \psi$  and Symmetric and Mirror left-right models as a function of  $M_{Z'}$  (and  $M_{A_H}$ ) for  $\sqrt{s} = 500$  GeV. Near the resonant region ( $\sqrt{s} = 500$

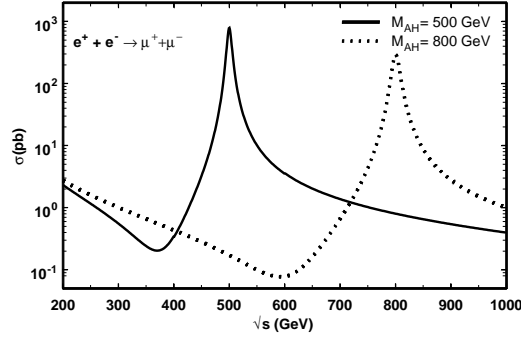


FIG. 1: Total cross section versus  $\sqrt{s}$  for  $M_{A_H} = 500$  and  $800$  GeV for LHM ( $c = 0.3$  and  $c' = 0.71$ ).

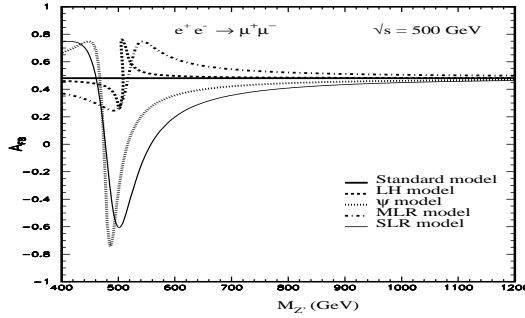


FIG. 2: Forward-backward asymmetry versus  $M_{Z'}$  ( $M_{A_H}$ ) for  $\sqrt{s} = 500$  GeV in  $e^+ + e^- \rightarrow \mu^+ + \mu^-$  for some models.

GeV) some models are more sensitive than the LHM, presenting sizeable deviations from the SM value  $A_{FB}^{SM} = 0.47$ . The same behavior occurs for  $\sqrt{s} = 1$  TeV. For larger values of the mass of the new gauge boson, the combined analysis of  $\mu$ ,  $c$  and  $b$  pair production might help to establish the best model underlying these deviations from the SM predictions.

Another variable that shows differences between models is the left-right asymmetry ( $A_{LR}$ ). The degrees of polarization of the electron and positron beams were taken to be 90% and 60% respectively. We present in Figures 5 for

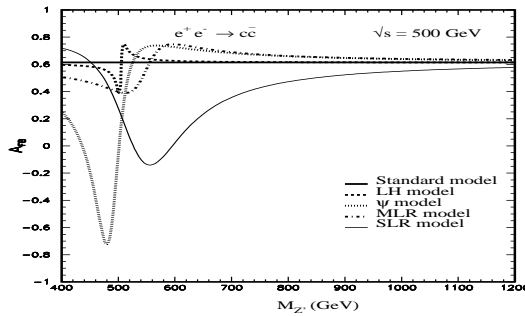


FIG. 3: Forward-backward asymmetry versus  $M_{Z'}$  ( $M_{A_H}$ ) for  $\sqrt{s} = 500$  GeV in  $e^+ + e^- \rightarrow c + \bar{c}$  for some models.

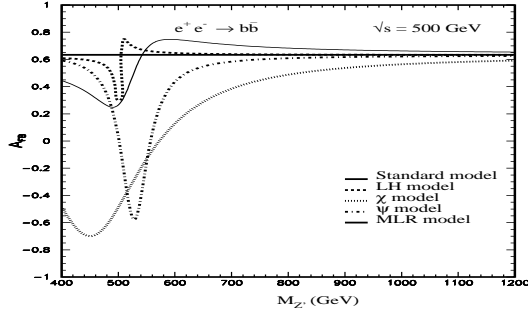


FIG. 4: Forward-backward asymmetry versus  $M_{Z'}$  ( $M_{A_H}$ ) for  $\sqrt{s} = 500$  GeV in  $e^+ + e^- \rightarrow b + \bar{b}$  for some models.

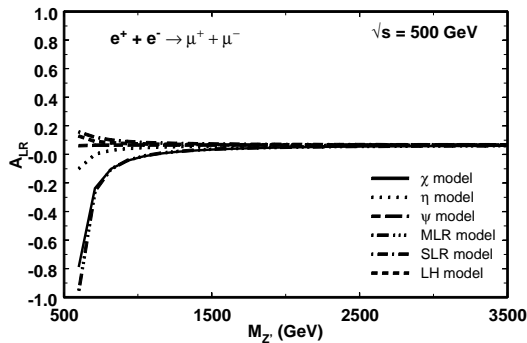


FIG. 5: Left-right asymmetry in  $e^+ + e^- \rightarrow \mu^+ + \mu^-$  versus  $M_{Z'}$  ( $M_{A_H}$ ) for  $\sqrt{s} = 500$  GeV for some models.

$\mu^+\mu^-$ , 6 for  $c\bar{c}$  and 7 for  $b\bar{b}$ , the left-right asymmetry for different models as a function of  $M_{Z'}$  for  $\sqrt{s} = 500$  GeV. Again the  $A_{LR}$  for the LHM has a small deviation from the SM value. The  $A_{LR}$  for all models has a smaller deviation from the SM than the  $A_{FB}$  for the corresponding models. The polarized beams will not improve the model distinction with respect to the unpolarized beams.

#### IV. NEW BOUNDS IN THE LITTLEST HIGGS MODEL

Bounds on the LHM were previously obtained in [3, 22, 25, 26] at the energy peak of the new neutral gauge boson production, using a combination of physical observables at that energy. Deviations from the SM predictions were shown to be within these bounds.

In this paper we present new bounds on the mass  $M_{A_H}$  of the new neutral gauge boson  $A_H$  as a function of  $\cos\theta'$ . These new bounds are derived from the angular distribution of the final-state fermion, by means of a  $\chi^2$  test. Assuming that the experimental data in the fermion-pair production will be described by the SM predictions, we defined a  $\chi^2$  estimator

$$\chi^2 = \sum_{i=1}^{n_b} \left( \frac{N_i^{SM} - N_i^{LHM}}{\Delta N_i^{SM}} \right)^2, \quad (2)$$

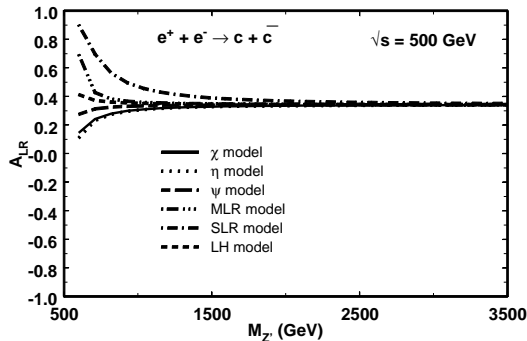


FIG. 6: Left-right asymmetry in  $e^+ + e^- \rightarrow c + \bar{c}$  versus  $M_{Z'}$  ( $M_{A_H}$ ) for  $\sqrt{s} = 500$  GeV for some models.

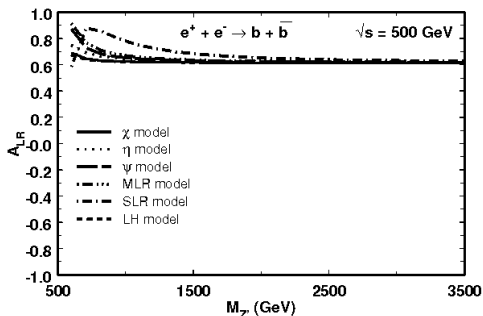


FIG. 7: Left-right asymmetry in  $e^+ + e^- \rightarrow b + \bar{b}$  versus  $M_{Z'}$  ( $M_{A_H}$ ) for  $\sqrt{s} = 500$  GeV for some models.

where  $N_i^{SM}$  is the number of SM events collected in the  $i^{th}$  bin,  $N_i^{LHM}$  is the number of events in the  $i^{th}$  bin as predicted by the LHM, and  $\Delta N_i^{SM} = \sqrt{(\sqrt{N_i^{SM}})^2 + (N_i^{SM}\epsilon)^2}$  the corresponding total error, which combines in quadrature the Poisson-distributed statistical error with the systematic error. We took  $\epsilon = 5\%$  as the systematic error in our calculation. We considered the muon, charm and bottom detection efficiencies equal to 95%, 60% and 35% respectively. We estimated upper bounds for  $M_{A_H}$  with 95% C.L., fixing  $c = 0.3$  and using the mixing angle  $\theta'$  as a free parameter. Figure 8 shows the bounds on  $M_{A_H}$ , for  $\sqrt{s} = 500$  GeV and an integrated luminosity  $\mathcal{L} = 100 \text{ fb}^{-1}$ . The 95% C.L. bounds for  $\sqrt{s} = 1 \text{ TeV}$  and  $\mathcal{L} = 340 \text{ fb}^{-1}$  are displayed in Figure 9. In both cases the muon channel was found to be more restrictive than the hadron channels.

In Figure 10 we display the resulting limits on  $M_{A_H}$  for  $\sqrt{s} = 500$  GeV, but considering longitudinally polarized beams. The degrees of polarization of the electron and positron beams were taken to be 90% and 60% respectively. The limits obtained in this case are less restrictive than the corresponding bounds derived from unpolarized angular distributions, and are essentially the same for all three final states.

## V. THE ASSOCIATED HARD PHOTON

A second point that can show interesting properties of a new fundamental interaction mechanism is the associated production of a general  $Z'$  and a hard photon in the process  $e^+ + e^- \rightarrow \gamma + f + \bar{f}$  [23]. This channel is suitable when  $M_{Z'} < \sqrt{s}$ . The main advantage of this channel is to show that one can study the new  $Z'$  properties before all



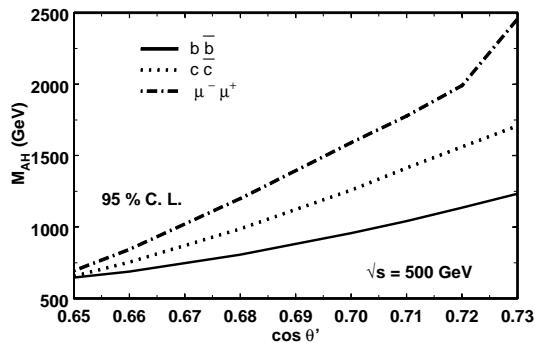


FIG. 8:  $M_{A_H}$  bounds (95% C.L.) as a function of  $\cos \theta'$  in  $e^+ + e^- \rightarrow f + \bar{f}$ , where  $f = \mu, c$  and  $b$  for  $\sqrt{s} = 500$  GeV for LHM.

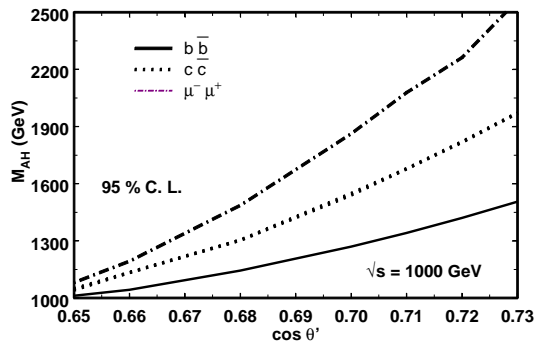


FIG. 9:  $M_{A_H}$  bounds (95% C.L.) as a function of  $\cos \theta'$  in  $e^+ + e^- \rightarrow f + \bar{f}$ , where  $f = \mu, c$  and  $b$  for  $\sqrt{s} = 1$  TeV for LHM.

the redefinition of the collider energy at the new neutral gauge boson mass. The total cross section for this channel is smaller than the direct resonant cross section but can give a statistically meaningful number of events, since the expected luminosity for the ILC will be larger than  $100 \text{ fb}^{-1}$ . Another important advantage is that one does not need to reconstruct the heavy neutral boson mass from its decay products. The direct  $Z'$  decay is important, but the reconstruction efficiency will reduce the total number of events, as discussed in [30]. This reconstruction can be more complicated when these new bosons decay into unstable particles, like hadrons.

The hard photon emission proposed in this paper is very different from the usual multiphoton emission accompanying  $Z'$  production. The well known logarithm corrections [28] were studied more recently [29] and imply changes at the  $Z'$  pole. But these corrections are different from the kinematics of two body final state in the associated hard photon production [23].

A very simple consequence of the conservation of energy and momentum, is that the final high energy hard photon has a fixed energy given by

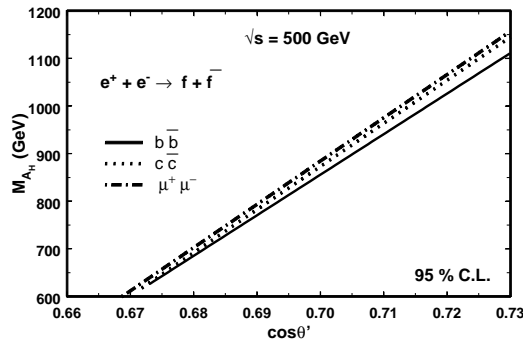


FIG. 10:  $M_{A_H}$  bounds (95% C.L.) as a function of  $\cos\theta'$  in  $e^+ + e^- \rightarrow f + \bar{f}$ , where  $f = \mu, c$  and  $b$  for  $\sqrt{s} = 500$  GeV for LHM, considering polarized beams.

$$E_\gamma \mp \Delta_\gamma = \frac{s - (M_{Z'} \pm \Delta_{Z'})^2}{2\sqrt{s}} \quad (3)$$

where  $\Delta_\gamma$  and  $\Delta_{Z'}$  are the uncertainties in the photon energy and  $M_{Z'}$ .

The study of the hard photon energy distribution will give the same information as the direct  $Z'$  decays, but in a simple and direct way since it is not necessary to reconstruct the  $Z'$  subproducts. The resulting photon energy distribution contains important information about the  $A_H$  and  $Z_H$  bosons and is shown in Figures 11 and 12, for the process  $e^+ + e^- \rightarrow \gamma + \mu^- + \mu^+$ . Similar results would be obtained for  $e^+ + e^- \rightarrow \gamma + e^- + e^+$ . For  $\sqrt{s} = 3$  TeV if  $M_{A_H} < 750$  GeV, the photon energy distribution  $d\sigma/dE_\gamma$  shows two peaks, coming from  $A_H$  and  $Z_H$ , when considering the LHM. For  $M_{A_H} > 750$  GeV only the peak associated to  $A_H$  will show up. The figures were obtained using a cut  $E_\gamma > 50$  GeV on the hard photon energy,  $E_j > 5$  GeV and  $|\cos\phi_i| < 0.995$ , where  $j = f, \bar{f}$  and  $i = \gamma, f, \bar{f}$ . The  $E_\gamma > 50$  GeV cut eliminates the contributions from the  $\gamma$ 's soft emissions.

We notice the strong mixing-angle dependence on the magnitude of the photon peaks in Figure 11. The peak associated to  $Z_H$  will depend on  $\cos\theta$  and the peak associated to  $A_H$  will vary with  $\cos\theta'$ . The  $\eta, \chi$  and  $\psi$  models have a much larger value for the total neutral gauge boson width and this fact makes the hard photon energy much broader as shown in Figure 12. The  $E_\gamma$  distribution allows us to find the  $Z'$  mass and to distinguish the models, in connection with Eq. (3).

## VI. CONCLUSIONS

We have shown that  $A_{FB}$  is better than  $A_{LR}$  in  $e^+ + e^- \rightarrow f + \bar{f}$ , where  $f = \mu, b$  and  $c$ , for  $M_{Z'} > \sqrt{s}$ , and can distinguish the LHM from other proposed models in a wide  $Z'$  mass range. A  $\chi^2$  analysis on the angular distribution of the final fermions for the same channels allows us to obtain a more restrictive  $Z'$  mass limits as a function of  $\cos\theta'$ . The above calculations were done considering polarized and unpolarized beams. Using the angular distribution it is possible to get other mass limits than using simply the total cross-sections as done by [25].

For  $M_{Z'} < \sqrt{s}$ , the hard photon energy distribution in  $e^+ + e^- \rightarrow \gamma + f + \bar{f}$  can indicate the theoretical origin of new possible heavy neutral gauge bosons independent of how these new bosons decay. This alternative signature for  $Z'$  production at the new electron-positron colliders could allow us to study its properties, at a fixed collider energy. If  $M_{A_H} < \sqrt{s} < M_{Z_H}$  only one peak shows up in the hard photon energy distribution, and the models can be

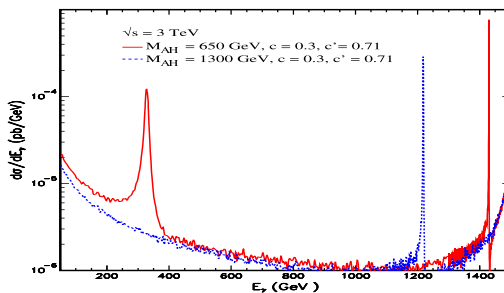


FIG. 11: Photon energy distribution in  $e^+ + e^- \rightarrow \gamma + \mu^- + \mu^+$  showing two peaks associated to  $M_{A_H} = 650$  GeV (third peak) and  $M_{Z_H} = 2600$  GeV (first peak) with  $\sqrt{s} = 3$  TeV for LHM ( $c = 0.3$  and  $c' = 0.71$ ), and only one (central) peak when  $M_{A_H} = 1300$  GeV.

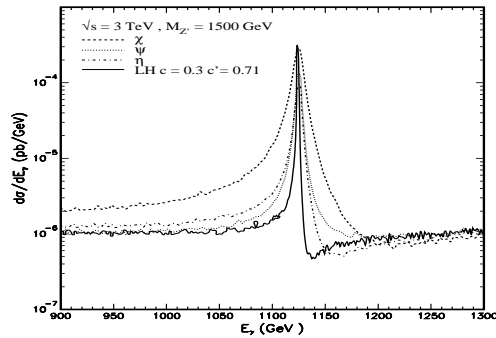


FIG. 12: Photon energy distribution in  $e^+ + e^- \rightarrow \gamma + \mu^- + \mu^+$  with  $\sqrt{s} = 3$  TeV for  $\chi$ ,  $\eta$ ,  $\psi$  and for LHM ( $c = 0.3$  and  $c' = 0.71$ ).

distinguished using the width of this peak. If  $M_{Z_H} < \sqrt{s}$  two peaks appear in the photon energy distribution, and all the models will be excluded, except the LHM.

In order to detect a new gauge boson and understand its properties, the center-of-mass energy of the future high-energy electron-positron experiments will have to be set to the mass of this new boson. The main point presented in our work is to show that we can establish the same properties of the possible new gauge boson when  $\sqrt{s} \neq M_{Z'}$  since the first periods of collider data taking, as shown in Figures 11 and 12.

*Acknowledgments:* This work was partially supported by the following Brazilian agencies: CNPq, FAPEMIG and FAPERJ.

- 
- [1] N. Arkani-Hamed, A. G. Cohen and H. Georgi, Phys. Lett. B **513**, 232 (2001). [arXiv:hep-ph/0105239].  
[2] N. Arkani-Hamed, A. G. Cohen, E. Katz and A. E. Nelson, JHEP **0207**, 034 (2002). [arXiv:hep-ph/0206021].  
[3] T. Han, H. E. Logan, B. McElrath and L. T. Wang, Phys. Rev. D **67**, 095004 (2003). [arXiv:hep-ph/0301040].  
[4] M. Schmaltz and D. Tucker-Smith, [arXiv:hep-ph/0502182].  
[5] M. Perelstein, [arXiv:hep-ph/0512128].  
[6] C. Csaki, J. Hubisz, G. D. Kribs, P. Meade and J. Terning, Phys. Rev. D **68**, 035009 (2003); T. Gregoire, D. R. Smith and J. G. Wacker, Phys. Rev. D **69**, 115008 (2004).  
[7] M. Perelstein, M. E. Peskin and A. Pierce, Phys. Rev. D **69**, 075002 (2004). [arXiv:hep-ph/0310039].

- [8] I. Low, JHEP **0410**, 067 (2004). [arXiv:hep-ph/0409025].
- [9] J. Hubisz and P. Meade, Phys. Rev. D **71**, 035016 (2005). [arXiv:hep-ph/0411264].
- [10] J. Hubisz, P. Meade, A. Noble and M. Perelstein, JHEP **0601**, 135 (2006). [arXiv:hep-ph/0506042].
- [11] F. Pisano and V. Pleitez, Phys. Rev. D **46**, 410 (1992).
- [12] P. H. Frampton, Phys. Rev. Lett. **69**, 2889 (1992).
- [13] N. Arkani-Hamed, A. G. Cohen and H. Georgi, Phys. Lett. B **513**, 232 (2001); N. Arkani-Hamed, A. G. Cohen, E. Katz and A. E. Nelson, JHEP **0207**, 034 (2002).
- [14] An extensive list of references can be found in R. N. Mohapatra and P. B. Pal, "Massive Neutrinos in Physics and Astrophysics", World Scientific, Singapore, 1998.
- [15] M. Cvetič, D. A. Demir, J. R. Espinosa, L. Everett and P. Langacker, Phys. Rev. **56**, 2861 (1997).
- [16] J. L. Hewett, T. G. Rizzo, Phys. Rep. **183**, 193 (1989).
- [17] T. G. Rizzo, e-Conference C040802, L013 (2004).
- [18] American Linear Collider Group, [arXiv:hep-ex/0106055 v1].
- [19] Physics at an  $e^+e^-$  Linear Collider, TESLA Technical Design Report, Part III, Eds. R. -D. Heuer, D. Miller, F. Richard, P. M. Zerwas, March 2001.
- [20] F. Abe et al., Phys. Rev. Lett. **79**, 2192 (1997); S. Obachi et al., Phys. Lett. B **385**, 471 (1996).
- [21] J. A. Conley, J. Hewett and M. P. Le, Phys. Rev. D **72**, 115014 (2005). [arXiv:hep-ph/0507198].
- [22] S. Godfrey, P. Kalyniak and A. Tomkins, [arXiv:hep-ph/0511335].
- [23] F. M. Almeida, Y. A. Coutinho, J. A. M. Simões, A. J. Ramalho, S. Wulck and M. A. B. do Vale, Eur. Phys. J. C **44** (2005) 127. [arXiv:hep-ph/0412395].
- [24] Particle Data Group, Phys. Lett. B **592**, (2004) 1.
- [25] Chong-Xing Hue, Wei Wang, Feng Zhang, Nucl. Phys. B **716**, (2005) 199. [arXiv:hep-ph/0409066].
- [26] Gi-Chol Cho and Aya Omote, Phys. Rev. D **70**, (2004) 057701.
- [27] A. Pukhov, E. Boos, M. Dubinin, V. Edneral, V. Ilyin, D. Kovalenko, A. Kryukov, V. Savrin, S. Shichanin and A. Semenov, "CompHEP"- a package for evaluation of Feynman diagrams and integration over multi-particle phase space. Preprint INP MSU 98-41/542 [arXiv:hep-ph/9908288]
- [28] O. Nicosini and L. Trentadue, Phys. Lett. B **196**, (1987) 551.
- [29] A. Freitas, Phys. Rev. D **70**, (2004) 015008.
- [30] X. Wang, Q. Zeng, Z. Jin and S. Liu, [arXiv:hep-ph/0702064].